Cell Reports
Medicine

Article

A targeted proteomics assay for the preoperative diagnosis of thyroid nodules

Graphical abstract

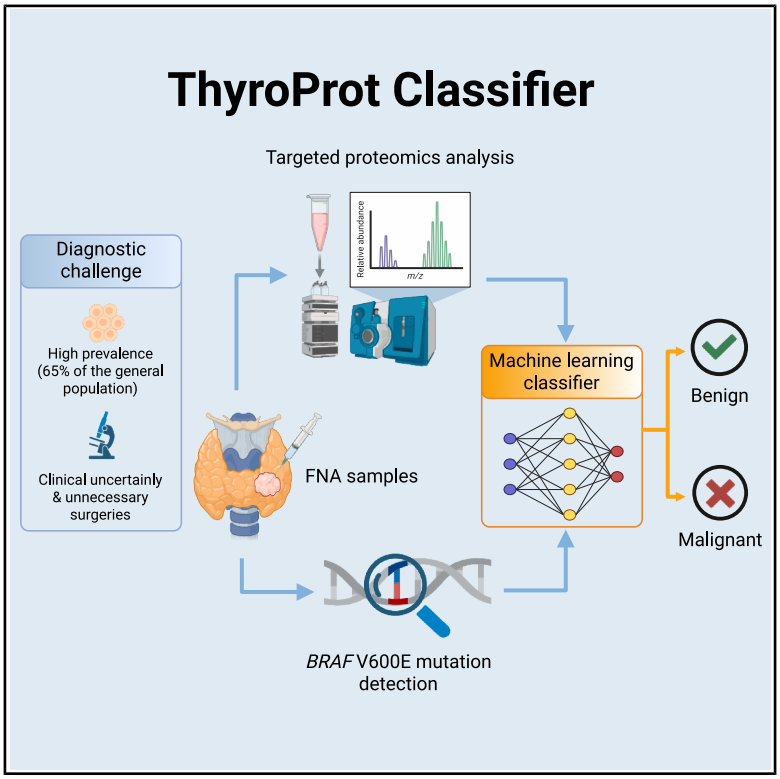

Authors

Xue Cai, Yaoting Sun, Dingcun Luo, ..., Yi Zhu, Yu Wang, Tiannan Guo

Correspondence

tianwen301_cta01@163.com (W.T.), xuhuixiong@126.com (H.X.), zhuyi@westlake.edu.cn (Y.Z.), neck130@sina.com (Y.W.), guotiannan@westlake.edu.cn (T.G.)

In brief

Cai et al. develop ThyroProt, a diagnostic classifier integrating targeted mass-spectrometry-based 3-protein quantification with *BRAF* V600E mutation, age, and gender for preoperative diagnosis of thyroid nodules, including indeterminate cases.

Highlights

- A mass-spectrometer-based targeted proteomics classifier
- Integration of protein expression and gene mutation for thyroid nodule diagnosis
- Preoperative diagnosis of thyroid nodules, including indeterminate cytology
- Real-world clinical validation in two prospective, blinded, multicenter cohorts

Cai et al., 2026, Cell Reports Medicine 7, 102664
March 17, 2026
https://doi.org/10.1016/j.xcrm.2026.102664

CellPress

Cell Reports Medicine

CellPress
OPEN ACCESS

Article

A targeted proteomics assay for the preoperative diagnosis of thyroid nodules

Xue Cai,[1,2,3,32] Yaoting Sun,[1,2,3,32] Dingcun Luo,[4,32] Hao Zhang,[5,32] Wenjun Wei,[6,7,32] Yifeng Zhang,[8,32] Weigang Ge,[9,32] Jing Liu,[10] Guan Ruan,[9] Lu Li,[1,2,3] Lingling Tan,[9] Luang Xu,[9] Dong Xu,[11] Haixia Guan,[12] Jiang Zhu,[13] Wanyuan Chen,[14] Qiushi Zhang,[9] Huijuan Si,[9] Juntao Qiu,[9] Zhangzhi Xue,[1,2,3] Zhiqiang Gui,[5] Haitao Zheng,[15] Gaosong Wu,[16]

(Author list continued on next page)

[1]Affiliated Hangzhou First People's Hospital, State Key Laboratory of Medical Proteomics, School of Medicine, Westlake University, Hangzhou, Zhejiang Province, China
[2]Westlake Center for Intelligent Proteomics, Westlake Laboratory of Life Sciences and Biomedicine, Hangzhou, Zhejiang, China
[3]Research Center for Industries of the Future, Westlake University, 600 Dunyu Road, Hangzhou, Zhejiang, China
[4]Department of Oncological Surgical, Affiliated Hangzhou First People's Hospital, School of Medicine, Westlake University, Hangzhou, Zhejiang, China
[5]Department of Thyroid Surgery, the First Hospital of China Medical University, Shenyang, Liaoning, China
[6]Department of Head and Neck Surgery, Fudan University Shanghai Cancer Center
[7]Department of Oncology, Shanghai Medical College, Fudan University, Shanghai, China
[8]Department of Medical Ultrasound, Shanghai Tenth People's Hospital, Tongji University School of Medicine, Shanghai, China
[9]Westlake Omics (Hangzhou) Biotechnology Co., Ltd., No.1, Yunmeng Road, Cloud Town, Xihu District, Hangzhou, Zhejiang, China
[10]First Hospital of Shanxi Medical University, Thyroid Surgery Department, Taiyuan, Shanxi, China
[11]Department of Ultrasound, Zhejiang Cancer Hospital, Hangzhou, Zhejiang, China
[12]Department of Endocrinology, Guangdong Provincial People's Hospital (Guangdong Academy of Medical Sciences), Southern Medical University, Guangzhou, China
[13]Women's Hospital, Zhejiang University School of Medicine, Hangzhou, Zhejiang, China
[14]Department of Pathology, Zhejiang Provincial People's Hospital, People's Hospital of Hangzhou Medical College, Hangzhou, Zhejiang, China
[15]Department of Thyroid Surgery, Affiliated Yantai Yuhuangding Hospital, Qingdao University, Shandong, China
[16]Department of Thyroid and Breast Surgery, Zhongnan Hospital of Wuhan University, 169 Donghu Road, Wuhan, Hubei, China
[17]Department of Thyroid and Breast Surgery, Affiliated Hospital of Integrated Chinese and Western, Nanjing University of Chinese Medicine, Nanjing, Jiangsu, China

(Affiliations continued on next page)

SUMMARY

Accurate preoperative diagnosis of thyroid nodules via fine-needle aspiration (FNA) biopsy remains challenging, particularly in cases with indeterminate cytology. This prospective, noninterventional, blinded, multicenter study establishes ThyroProt, a diagnostic classifier that integrates targeted mass-spectrometry-based quantification of a 3-protein signature with *BRAF* V600E mutation status, age, and gender. Developed and validated on 837 FNA samples, the classifier is evaluated in a prospective test set of 322 samples, achieving an area under the curve (AUC) of 0.94 with an overall accuracy of 90.7%. For the critical subgroup of Bethesda III/IV nodules, ThyroProt demonstrates an accuracy of 88.0%, with 82.4% sensitivity and 100% specificity. The classifier's robust performance is further evaluated in two independent multicenter cohorts, where it maintains an AUC of 0.87–0.91 and an accuracy of 84.3%–85.7%. This study supports the clinical utility of mass-spectrometry-based targeted proteomics for improving preoperative diagnosis of thyroid nodules, particularly those with indeterminate cytology.

INTRODUCTION

The prevalence of thyroid nodules has been reported as high as 65% of the general population.[1,2] Fine-needle aspiration (FNA) biopsy is the current diagnostic mainstay for thyroid nodules, providing reliable diagnosis in most cases.[3–5] However, diagnostic challenges persist, particularly for indeterminate cytology classified as Bethesda III, IV, or V.[4,6,7] The rates of malignancy (ROMs) associated with these cytological categories typically range from 13% to 30%, 23% to 34%, and 67% to 83%,

Jianhua Wang,[17] Lei Xie,[18] Guang Chen,[19] Guoyang Wu,[20] Lei Liang,[21] Chuang Chen,[22] Xianghui He,[23] Meiping Shen,[24] Jianbiao Wang,[18] Minghua Ge,[14] Deguang Zhang,[18] Liang Zhou,[18] Yijun Wu,[25] Hui Shi,[8] Fan Wu,[4] Zhihong Wang,[5] Hong Han,[26] Jing Yao,[27] Zhiyan Liu,[28] Mingzhao Xing,[29] Kennichi Kakudo,[30] Yibo Gao,[31] Wen Tian,[27,*] Huixiong Xu,[26,*] Yi Zhu,[1,2,3,*] Yu Wang,[6,7,*] and Tiannan Guo[1,2,3,33,*]

[18]Department of Head and Neck surgery, Institute of Micro-Invasive Surgery of Zhejiang University, The Affiliated Sir Run Run Shaw Hospital, School of Medicine, Zhejiang University, Hangzhou, Zhejiang, China
[19]Department of Thyroid Surgery, General Surgery Center, The First Hospital of Jilin University, Changchun, Shenyang, China
[20]Department of General Surgery, Zhongshan Hospital Affiliated with Xiamen University, Xiamen, China
[21]Department of Ultrasound, Aerospace Center Hospital, Beijing, China
[22]Department of Breast and Thyroid Surgery, Renmin Hospital of Wuhan University, Wuhan, Hubei, China
[23]Department of General Surgery, Tianjin Medical University General Hospital, Tianjin, China
[24]Department of General Surgery, the First Affiliated of Nanjing Medical University, Nanjing, Jiangsu, China
[25]Department of Thyroid Surgery, The First Affiliated Hospital, School of Medicine, Zhejiang University, Hangzhou, China
[26]Department of Ultrasound, Zhongshan Hospital, Institute of Ultrasound in Medicine and Engineering, Fudan University, Shanghai, China
[27]Department of Thyroid & Hernia Surgery, Medical Department of General Surgery, The First Medical Center of Chinese People's Liberation Army General Hospital, Beijing, China
[28]Department of Pathology, Shanghai Sixth People's Hospital Affiliated to Shanghai Jiao Tong University School of Medicine, Shanghai, China
[29]School of Medicine, Southern University of Science and Technology, Shenzhen, Guangdong, China
[30]Department of Pathology, Cancer Genome Center and Thyroid Disease Center, Izumi City General Hospital, Izumi, Japan
[31]Central Laboratory & Shenzhen Key Laboratory of Epigenetics and Precision Medicine for Cancers, National Cancer Center/National Clinical Research Center for Cancer/Cancer Hospital & Shenzhen Hospital, Chinese Academy of Medical Sciences and Peking Union Medical College, Shenzhen 518116, China
[32]These authors contributed equally
[33]Lead contact
*Correspondence: tianwen301_cta01@163.com (W.T.), xuhuixiong@126.com (H.X.), zhuyi@westlake.edu.cn (Y.Z.), neck130@sina.com (Y.W.), guotiannan@westlake.edu.cn (T.G.)
https://doi.org/10.1016/j.xcrm.2026.102664

respectively.[6] There remains an on-going critical clinical need to develop molecular tests for more precise and accurate diagnosis of these cytologically indeterminate thyroid nodules.[8–10]

To address this issue, multiple molecular diagnostic tests have been developed.[11,12] The *BRAF* V600E mutation test in the preoperative FNA specimen is significantly correlated with poor clinical pathological results and mortality rate in papillary thyroid cancer (PTC).[13,14] However, overall, for indeterminate thyroid nodules, a meta-analysis showed the sensitivity of *BRAF* V600E mutation analysis to be only about 40% in Western patient cohorts where *BRAF* V600E-mutated PTCs are few in indeterminate thyroid nodules.[15] The quantitative variant allele fraction (VAF) assays of *BRAF* V600E and TERT promoter have achieved a sensitivity and a specificity of 93.8 and 90%, respectively, for diagnosing indeterminate thyroid nodules.[16] Some nucleic-acid-based tests, such as Afirma[5,17,18] and ThyroSeq,[19–22] as well as imprinted genes of *SNRPN* and *HM13*[23] have improved the current clinical practice. Gene mutations are heterogeneous in different individuals and intra-tumor genomic heterogeneity is widely present. A new molecular diagnostic approach needs to be pursued and tested, such as protein classifier, combining genomics and proteomics, that may overcome these limitations and help improve the diagnosis of thyroid nodules.

Proteomics analysis of tumor specimens reveals information not only from the tumor cells but also from their microenvironments, which can differ between benign and malignant conditions. Protein samples are less susceptible to spontaneous degradation in clinical specimens. There are intense interests and increasing activities using proteomics to discover novel biomarkers for cancer diagnosis and prognosis. Thus, the current work aims to add a proteomic panel for offering an assay to determine the thyroid malignancy. A pressure cycling technology (PCT) protocol has been developed for proteomic analysis of tissue biopsy samples.[24,25] This technology is applicable in minimal amounts of both fresh-frozen tissue and formalin-fixed paraffin-embedded (FFPE) tissues. We have previously developed a classifier of 19 proteins for diagnosis of thyroid nodules, achieving a diagnostic accuracy of 91% in an internal retrospective cohort of 1724 samples, an accuracy of 89% in an independent retrospective cohort of 288 FFPE samples, and 85% in a prospective cohort of 294 FNA samples from 12 medical centers.[26] However, the previous data were collected by an untargeted method known as data independent acquisition mass spectrometry (DIA-MS) method with a 60-min gradient, which is relatively costly for clinical application. Targeted proteomics with higher accuracy, stability, and shorter gradients are more suitable for clinical applications. Coupled with synthesized stable isotope-labeled peptides (called AQUA peptides),[27] the absolute quantitative value of protein can be measured, eliminating batch effect.

To further improve the clinical utility of proteomics, based on previous data, a targeted proteomic method was performed in this study. Because the *BRAF* V600E-mutated PTCs constitute the majority of thyroid malignancy in Asian patient cohorts,[28,29] to improve the performance of the classifier, we developed a diagnostic protein classifier called ThyroProt, combining the analysis and expression of three proteins together with determination of *BRAF* V600E status, for the diagnosis of thyroid nodules. We initially developed and tested this assay across 15 medical centers, followed by two independent tests in two additional medical centers.

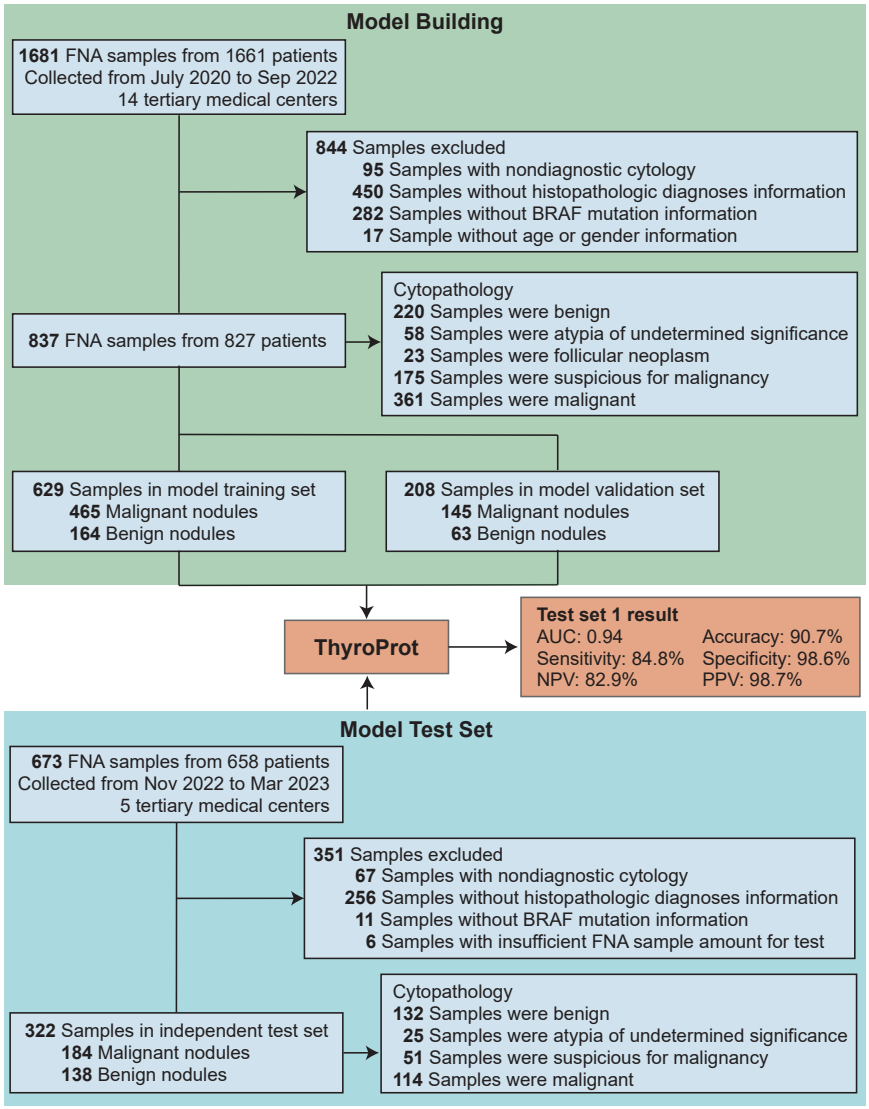

Figure 1. Recruitment and exclusion of samples for the classifier building and test in the study

Different samples from the same patient were derived from different nodules.

RESULTS

Training and validation of the ThyroProt

We collected 2,108 FNA samples from 2,072 patients at 14 tertiary medical centers from January 2020 to September 2022 of continuous enrollment for feature selection, model training, and validation (Table S1). Starting with 212 candidate proteins identified from preliminary research,[26] we developed and optimized a high-sensitivity targeted proteomics workflow to quantify 121 proteins. Machine learning analysis of 820 targeted proteomic datasets from 620 samples across 13 hospitals refined the panel to 38 diagnostically relevant proteins. Implementing a stable isotope-labeled reference peptide system enabled absolute quantification, which was applied to 1,312 clinical samples from 12 centers. Through iterative model optimization and rigorous performance evaluation of heavy peptides, three signature peptides derived from fibronectin (FN1), heat shock protein beta-1 (HSPB1), and protein S100-A6 (S100A6) were ultimately selected to construct a robust diagnostic model for thyroid nodule classification (Table S2).

After feature selection, 1,681 of 2,108 samples from 1,661 patients were acquired by MS mixed with AQUA peptides (Table S2B). A total of 844 samples were excluded, including 95 samples with nondiagnostic cytology, 450 samples without diagnostic histopathology confirmation, 282 samples for missing *BRAF* V600E mutation data, and 17 samples for missing age or gender information (Figure 1). The remaining 837 FNA samples from 827 patients were used for model training and validation: 220 were benign, 58 were atypia of undetermined significance, 23 were follicular neoplasm, 175 were suspicious for malignancy, and 361 were malignant (Figure 1; Tables 1 and S2C). Among them, 610 FNA samples were confirmed as malignant through surgery, 18 FNA samples were confirmed as benign by surgery, and the remaining cases were followed-up without histological confirmation (Table 1). The 208 FNA samples reported as Bethesda II or did not require surgery during the follow-up period[30] were also regarded as benign samples. In summary, 610 malignant samples were labeled as positive in model building, while other 227 samples were labeled as negative (Figure 1).

Of 837 FNA samples from thyroid nodules of 827 patients for model building, 629 were randomly selected for model training, while 208 were randomly selected for model validation (Tables S2B and S2D). The characteristics of the two groups were shown in the Table 1. In addition to *BRAF* V600E mutation information, the classifier model (ThyroProt) combines the absolute quantitative data measured by MS of three proteins with age and gender. The missing values for the three protein datasets are shown in Table S2D. More details of the model construction are provided in Methods.

The ThyroProt improves the area under the curve (AUC), accuracy, and sensitivity while maintaining high specificity compared to *BRAF* V600E mutation, especially for indeterminate thyroid nodules. In the diagnosis of thyroid FNA, compared with *BRAF* mutation, the AUC of the ThyroProt increased from 0.83 to 0.89, and the accuracy increased from 80.3% to 82.2%

Table 1. Clinical characteristics of the study subjects for model building and test set

	Model training	Model validation	Model test	Model independent test set 1	Model independent test set 2
Patient characteristic	623	207	313	230	42
Patient Gender					
Male, no. (%)	162 (26.0%)	48 (23.2%)	90 (28.8%)	57 (24.8%)	7 (16.7%)
Female, no. (%)	461 (74.0%)	159 (76.8%)	223 (71.2%)	173 (75.2%)	35 (83.3%)
Patient Age, Years					
Median	45	46	45	45	50
IQR	34.5–51.5	38–55	36–56	36–55	39–59
Sample characteristic	629	208	322	230	51
Start date of sample collection	20200715	20200902	20221101	–	–
End date of sample collection	20220613	20220912	20230310	–	–
BARF Mutation					
Non-mutation, no. (%)	244 (38.8%)	92 (44.2%)	169 (52.5%)	109 (47.4%)	38 (74.5%)
Mutation, no. (%)	385 (61.2%)	116 (55.2%)	153 (47.5%)	121 (52.6%)	13 (25.5%)
Mutation in malignant, no. (%)	379 (81.5%)	110 (75.9%)	151 (82.1%)	116 (81.7%)	11 (57.9%)
Mutation in Bethesda III cytology, no. (%)	2 (66.7%)	33 (60.0%)	13 (52.0%)	6 (21.4%)	1 (25.0%)
Bethesda Classification					
II	167 (26.6%)	53 (25.5%)	132 (41.0%)	31 (13.5%)	31 (60.8%)
III	3 (0.5%)	55 (26.4%)	25 (7.8%)	28 (12.2%)	4 (7.8%)
IV	2 (0.3%)	21 (10.1%)	0 (0%)	34 (14.8%)	0 (0%)
V	143 (22.7%)	32 (15.4%)	51 (15.8%)	56 (24.3%)	3 (5.9%)
VI	314 (49.9%)	47 (22.6%)	114 (35.4%)	81 (35.2%)	13 (25.5%)
Benign nodules, no. (%)	164 (26.1%)	63 (30.2%)	138 (42.9)	89 (38.7%)	32 (62.7%)
Surgically confirmed cases	8	10	7	15	1
MNG	7	7	6	9	1
FA	1	1	0	6	0
HT	0	2	1	31	28
[a]Bethesda II	156	52	126	43	3
[b]Benign during follow-up	0	1	5	141 (61.3%)	19 (37.3%)
Malignant nodules, no. (%)	465 (73.9%)	145 (69.7%)	184 (57.1%)	141	19
Surgically confirmed cases	465	145	184	141	19
PTC	462	143	183	–	–
FTC	0	2	1	–	–
PDTC	2	0	0	–	–
MTC	1	0	0	–	–

Abbreviations: PTC, papillary thyroid cancer; FTC, follicular thyroid carcinoma; PDTC, poorly differentiated thyroid cancer; MTC, medullary thyroid cancer; MNG, multinodular goiter; HT, Hashimoto's disease; FA, follicular adenoma.
[a]Bethesda II thyroid nodules that were not operated were included as benign FNA samples.
[b]Benign during follow-up represented cases that surgery would not have been required according to clinical guidelines.

(Figure 2A; Table S4). In the diagnosis of indeterminate nodules (Bethesda III–V), the AUC increased from 0.83 to 0.87 and the accuracy increased from 76.9% to 82.4%. While maintaining a specificity of 90.0%, the sensitivity increased from 75.5% to 81.6% (Table S4). The performance of ThyroProt model demonstrates a significant improvement in the diagnosis of Bethesda III and IV nodules. The AUC and accuracy increased from 0.78 to 0.83 and 69.7% to 76.3%, respectively (Figure 2A; Table S4). It is noteworthy that while maintaining a specificity of 88.9%, the sensitivity remarkably increased from 67.2% to 74.6% (Table S4).

Performance of ThyroProt in thyroid nodules

We also collected 673 FNA samples from 658 patients at five tertiary medical centers from November 2022 to March 2023 of continuous enrollment for test set (Figure 1; Tables S1 and S3A). A total of 351 samples were excluded, including 67 samples with nondiagnostic cytology, 256 samples without diagnostic histopathology confirmation, 11 samples for missing *BRAF* V600E mutation data, and 6 samples with insufficient FNA sample amount for test (Figure 1). The remaining 322 FNA samples were used for model test: 132 were benign, 25 were atypia of undetermined significance, 51 were suspicious for

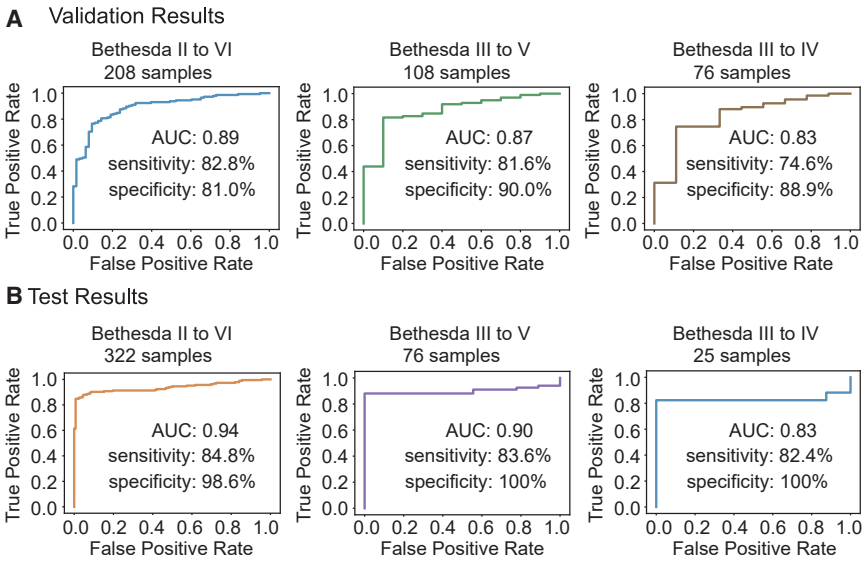

Figure 2. Performance of ThyroProt in the model validation and test set

ROC plots for (A) the validation results, containing the entire cohort, the samples reported as Bethesda III to V nodules, and the samples reported as Bethesda III or IV nodules; (B) test results, containing the entire cohort, the samples reported as Bethesda III to V nodules, and the samples reported as Bethesda III or IV nodules.

malignancy, and 114 were malignant (Figure 1; Table S3A). Among them, 184 FNA samples were confirmed as malignant through surgery, 7 FNA samples were confirmed as benign by surgery, and the remaining cases were followed-up without histological confirmation. The 131 FNA samples reported as Bethesda II or did not require surgery during the follow-up period[30] were also regarded as benign samples (Table S3A).

We tested the model using the prospective test set of 322 samples (Tables 1 and S3B) and achieved an AUC of 0.94 (Figure 2B) and a diagnostic accuracy of 90.7% (95% confidence interval [CI], 90.6–90.7). The targeted protein expression level of benign and malignant samples in the test set is shown in Figure S1A. The model correctly identified 156 out of the 184 malignant samples, corresponding to a sensitivity of 84.8% (95% CI, 79.6–90.0), and correctly identified 136 out of the 138 benign samples corresponding to a specificity of 98.6% (95% CI, 96.6–100). The positive predictive value (PPV) and negative predictive value (NPV) were 98.7% (95% CI, 97.0–100) and 82.9% (95% CI, 77.2–88.7), respectively. The diagnostic performance of the proteomic model is summarized in Table 2.

Among the 187 patients who underwent thyroidectomy, six were diagnosed as benign in postoperative histopathological examination. The classifier correctly diagnosed six benign samples, which could potentially help avoiding unnecessary surgeries for these six patients (Table S5). On the other hand, of the 158 test-positive samples in the study cohort, two (1.3%) were found to be false-positive, from two Bethesda II cytology nodules (Table S6). One out of the two false-positive samples was from the patient who did not undergo surgery. Another sample was from a patient with multiple thyroid nodules, which contains either benign nodule or PTC nodule, hence the diagnosis might be subject to interference from sampling accuracy.

Of the 164 test-negative samples, 28 (17.1%) were found to be false-negative, including samples from 1 Bethesda II cytology nodules, 3 Bethesda III cytology nodules, 8 Bethesda V cytology nodules, and 16 Bethesda VI cytology nodules (Table S6). The cytological pathology of Bethesda II samples is completely opposite to the histopathological results of PTC, which may be due to the inaccurate biopsy sampling. And other 18 samples were identified low-risk PTMC, with tumor diameter <1.0 cm, no local invasion, no cervical lymph node metastasis, and no high-grade PTC subtypes observed during biopsy, which meets the indication for active follow-up monitoring.[7,30] The remaining samples were classified as T1 or T2 (<2.2 cm, median 1.6 cm, interquartile range [IQR] 1.5–1.9 cm), intrathyroidal, and showed no signs of vascular invasion or clinical indications of distant metastasis. Whether these samples require immediate surgical removal or are more suitable for active follow-up monitoring or thermal ablation, further discussion is needed.

Performance of ThyroProt in indeterminate thyroid nodules

We also evaluated the performance of the ThyroProt on 76 indeterminate thyroid nodules reported as Bethesda III, IV, or V from the above test set, including 9 benign and 67 malignant tumors. Among the 67 surgery-confirmed malignant tumors, 56 were correctly classified as malignant. Similarly, nine benign nodules were all correctly classified as benign. This resulted in an AUC of 0.90 (Figure 2B) and a diagnostic accuracy of 85.5% (95% CI, 85.2–85.8), with a sensitivity, specificity, PPV, and NPV of 83.6% (95% CI, 74.7–92.5), 100% (95% CI, 100–100), 100% (95% CI, 100–100), and 45% (95% CI, 23.2–66.8), respectively (Table 2).

In the test set, there were 25 thyroid nodules reported as Bethesda III, including 8 benign and 17 malignant tumors. Among the 17 surgery-confirmed malignant tumors, 14 were correctly classified as malignant, while 8 benign nodules were all correctly classified as benign, resulting in an AUC of 0.83 (Figure 2C) and a diagnostic accuracy of 88.0% (95% CI, 87.2–88.8), with sensitivity, specificity, PPV, and NPV being 82.4% (95% CI, 64.2–100), 100% (95% CI, 100–100), 100% (95% CI, 100–100), and 72.7% (95% CI, 46.4–99.0), respectively (Table 2). Among eight benign cases correctly tested by the classifier model, three were confirmed benign by surgery, while five had follow-up information and were determined to be benign clinically during the follow-up time.

Performance of ThyroProt in two independent test sets

For the independent test set 1, we collected 954 FNA samples from 947 patients at one independent medical center

Table 2. Performance of the protein classifier (ThyroProt) on FNA samples of different Bethesda categories of thyroid nodule in the prospective test set

Variable	Bethesda II to VI nodules		Bethesda III to V nodules		Bethesda III & IV nodules	
Protein classifier result	malignant	benign	malignant	benign	malignant	benign
Malignant/positive, no.	156	2	56	0	14	0
Benign/negative, no.	28	136	11	9	3	8
AUC	0.94		0.90		0.83	
Accuracy, % (95% CI)	90.7 (90.6–90.7)		85.5 (85.2–85.8)		88.0 (87.2–88.8)	
Sensitivity, % (95% CI)	84.8 (79.6–90.0)		83.6 (74.7–92.5)		82.4 (64.2–100)	
Specificity, % (95% CI)	98.6 (96.6–100)		100 (100–100)		100 (100–100)	
PPV, % (95% CI)	98.7 (97.0–100)		100 (100–100)		100 (100–100)	
NPV, % (95% CI)	82.9 (77.2–88.7)		45.0 (23.2–66.8)		72.7 (46.4–99.0)	

(Figure 3A; Tables S1 and S3C). A total of 724 samples were excluded, including 130 samples with nondiagnostic cytology, 528 samples without diagnostic histopathology confirmation, one sample for missing *BRAF* V600E mutation data, and 65 samples with insufficient FNA sample amount for test (Figure 3A). The remaining 230 FNA samples were used for model test: 31 were benign, 28 were atypia of undetermined significance, 34 were follicular neoplasm, 56 were suspicious for malignancy, and 81 were malignant (Figure 3A; Table S3C). Among them, 141 FNA samples were confirmed as malignant through surgery, 15 FNA samples were confirmed as benign by surgery, and the 74 FNA samples reported as Bethesda II or did not require surgery during the follow-up period[30] were also regarded as benign samples (Table S3A).

Utilizing the independent test set 1 of 230 samples (Tables 1 and S3D), ThyroProt achieved an AUC of 0.91 (Figure 4A) and a diagnostic accuracy of 85.7% (95% CI, 85.5–85.8). The targeted protein expression level of benign and malignant samples in the independent test set 1 is shown in Figure S1B. The model correctly identified 120 out of the 141 malignant samples, yielding a sensitivity of 85.1% (95% CI, 79.2–91.0) and correctly identified 77 out of the 89 benign samples corresponding to a specificity of 86.5% (95% CI, 79.4–93.6) (Table 3). The PPV and NPV were 90.9% (95% CI, 86.0–95.8) and 78.6% (95% CI, 70.4–86.7), respectively (Table 3). Among the 156 patients who underwent thyroidectomy, 15 were diagnosed as benign in postoperative histopathological examination. The classifier correctly diagnosed 13 of 15 benign samples, which could have potentially helped avoiding unnecessary surgeries for these six patients (Table S7). On the other hand, of the 132 test-positive samples in the study cohort, 12 (9%) were found to be false-positive, from six Bethesda II cytology nodules, two Bethesda III cytology nodules, three Bethesda IV cytology nodules, and one Bethesda VI cytology nodule (Table S7). Ten out of the twelve false-positive samples were from the patient who did not undergo surgery. And in the 230 FNA test samples, only 14.3% were labeled as containing a large amount of colloid, and among these 10 samples, 7 (70.0%) contained a significant amount of colloid, which could be one of the factors affecting the results. The remaining two FNA samples showed cytopathological evidence of cancer cells, but postoperative pathology diagnosed them as thyroid nodules, which may be related to the radiofrequency ablation the two patients underwent prior to surgery. Of the 98 test-negative samples, 21 (21.4%) were found to be false-negative, including samples from 2 Bethesda III cytology nodules, 9 Bethesda V cytology nodules, and 10 Bethesda VI cytology nodules (Table S7). Between them, 15 samples were identified low-risk PTMC, with tumor diameter <1.0 cm, no local invasion, no cervical lymph node metastasis, and no high-grade PTC subtypes observed during biopsy, which meets the indication for active follow-up monitoring.[7,30] The remaining samples were classified as T1 (<2 cm, median 1.7 cm, IQR 1.4–1.9 cm), intrathyroidal, and showed no signs of vascular invasion or clinical indications of distant metastasis.

For the independent test set 2, we collected 253 FNA samples from 214 patients at another independent medical center (Figure 3A; Tables S1 and S3E). A total of 202 samples were excluded, including 165 samples with nondiagnostic cytology, 14 samples without diagnostic histopathology confirmation, 18 samples for missing *BRAF* V600E mutation data, and 5 samples with insufficient FNA sample amount for test (Figure 3B). The remaining 51 FNA samples were used for model test: 31 were benign, 4 were atypia of undetermined significance, 3 were suspicious for malignancy, and 13 were malignant (Figure 3B; Table S3E). Among them, 19 FNA samples were confirmed as malignant by surgery, 1 FNA sample was confirmed as benign by surgery, and the 31 FNA samples reported as Bethesda II or did not require surgery during the follow-up period[30] were also regarded as benign samples (Table S3E).

For the independent test set 2 comprising 51 samples (Tables 3 and S3F), ThyroProt achieved an AUC of 0.87 (Figure 4D) and a diagnostic accuracy of 84.3% (95% CI, 83.8–84.8). The targeted protein expression level of benign and malignant samples in the independent test set 1 is shown in Figure S1C. The model accurately identified 11 out of the 17 malignant samples, yielding a sensitivity of 64.7% (95% CI, 42.0–87.4), and correctly identified 32 of 34 benign samples corresponding to a specificity of 94.1% (95% CI, 86.2–100) (Table 3). The PPV and NPV were 84.6% (95% CI, 65.0–100) and 84.2% (95% CI, 72.6–95.8), respectively (Table 3). Among the 20 patients who underwent thyroidectomy, one was diagnosed as benign in postoperative histopathological examination. The classifier correctly diagnosed this benign sample, which could have potentially helped avoiding unnecessary surgery

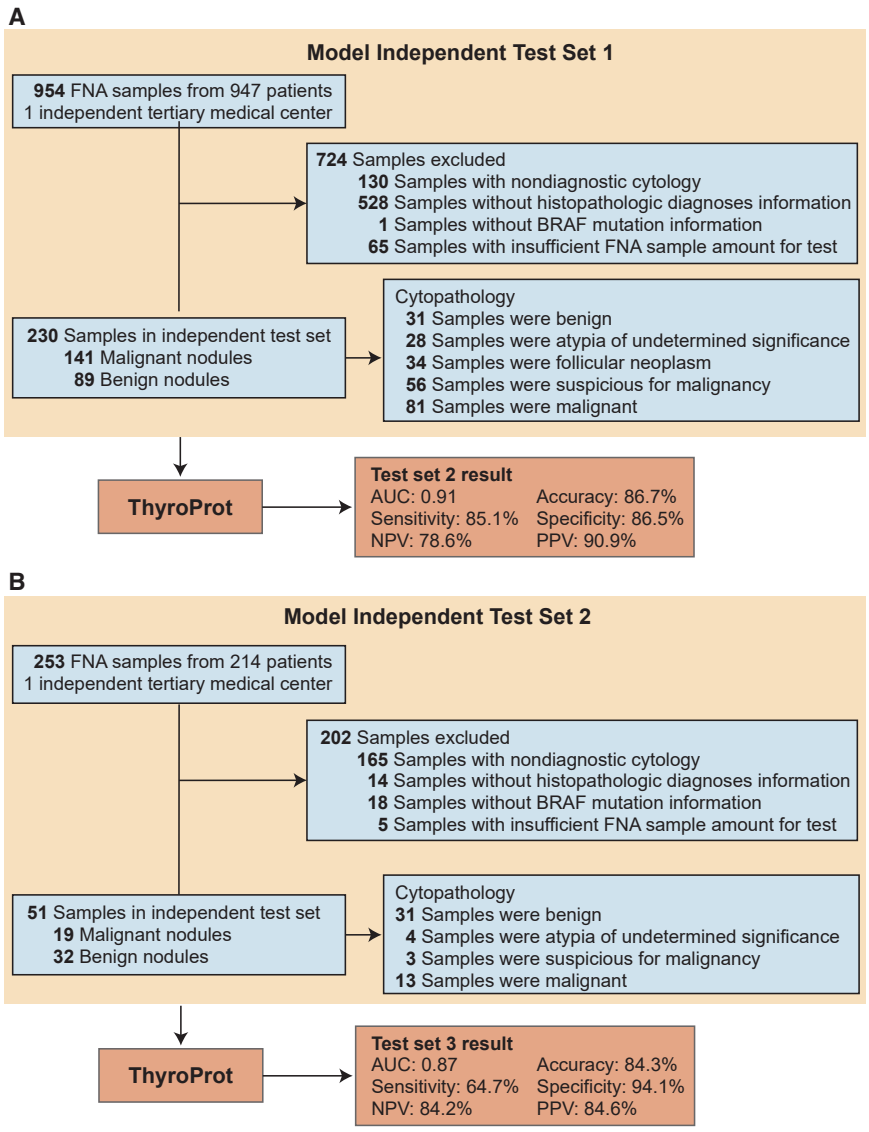

Figure 3. Recruitment and exclusion of samples for the two independent test sets from two independent medical centers

Different samples from the same patient were derived from different nodules.

(A) The first independent test set for the classifier.

(B) The second independent test set for the classifier.

Performance of ThyroProt in indeterminate thyroid nodules of the independent test set

We also evaluated the ThyroProt on 118 indeterminate thyroid nodules reported as Bethesda III, IV, or V from the independent test set 1, comprising 57 benign and 61 malignant tumors. Out of 61 surgery-confirmed malignant tumors, 50 were correctly classified as malignant, and 52 of 57 benign nodules were correctly classified. This resulted in an AUC of 0.89 (Figure 4B) and a diagnostic accuracy of 86.4% (95% CI, 86.2–86.6). Sensitivity, specificity, PPV, and NPV were 82.0% (95% CI, 72.3–91.6), 91.2% (95% CI, 83.9–98.6), 90.9% (95% CI, 83.3–98.5), and 82.5% (95% CI, 73.2–91.9), respectively (Table 3).

There were 62 thyroid nodules reported as Bethesda III or IV in the independent test set 1, comprising 53 benign and 9 malignant tumors. Of the nine surgery-confirmed malignant tumors, seven were correctly classified as malignant, while 48 out of 53 benign nodules were correctly classified as benign, resulting in an AUC of 0.93 (Figure 4C) and a diagnostic accuracy of 88.7% (95% CI, 88.4–89.0) and the sensitivity, specificity, PPV, and NPV being 77.8% (95% CI, 50.6–100), 90.6% (95% CI, 82.7–98.4), 58.3% (95% CI, 30.4–86.2), and 96.0% (95% CI, 90.6–100), respectively (Table 3). Among 48 benign cases correctly tested by the classifier model, 10 were confirmed benign by surgery, while 38 had follow-up information and were determined to be benign clinically during the follow-up time (Table S7).

(Table S8). On the other hand, of the 13 test-positive samples in the study cohort, 2 (15.4%) were found to be false-positive, from one Bethesda II cytology nodule and one Bethesda III cytology nodule (Table S8), which were from the patient who did not undergo surgery. One of the samples was from a patient with multiple thyroid nodules, including malignant and benign thyroid nodules. Of the 38 test-negative samples, 6 (15.8%) were found to be false-negative, including samples from one Bethesda III cytology nodule, one Bethesda V cytology nodule, and four Bethesda VI cytology nodules (Table S8). Between them, four samples were identified low-risk PTMC, with tumor diameter <1.0 cm, no local invasion, no cervical lymph node metastasis, and no high-grade PTC subtypes observed during biopsy, which meets the indication for active follow-up monitoring.[7,30] The remaining samples were classified as T1, intrathyroidal, and showed no signs of vascular invasion or clinical indications of distant metastasis.

DISCUSSION

In this study, we combined MS-based targeted protein expression analysis and *BRAF* V600E mutation data along with age and gender to establish an integrative classifier for the diagnosis of thyroid nodules. Specifically, the classifier achieved an AUC of 0.94, an accuracy of 90.7%, a sensitivity of 84.8% and a specificity of 98.6%, with a PPV and NPV of 98.7% and 82.9%, respectively. The test was also superior for the Bethesda III and IV thyroid nodules, achieving an AUC of 0.83, an accuracy

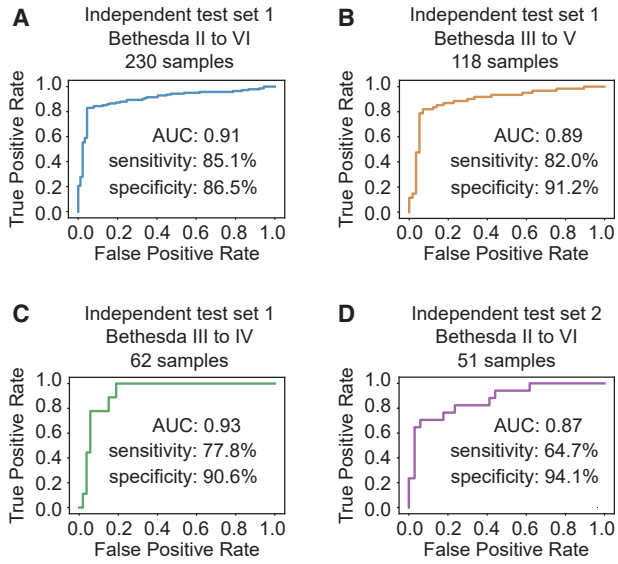

Figure 4. Performance of ThyroProt in two independent test sets

ROC plots for (A) the entire cohort in the independent test set 1; (B) the samples reported as Bethesda III to V nodules in the independent test set 1; (C) the samples reported as Bethesda III or IV nodules in the independent test set 1; (D) the entire cohort in the independent test set 2.

of 88.0%, a sensitivity of 82.4%, a specificity of 100%, a PPV of 100% and an NPV of 72.7%. For two independent test sets from two independent medical centers, the classifier achieved an AUC of 0.87%–0.91%, an accuracy of 84.3%–85.7%, a sensitivity of 64.7%–85.1%, and a specificity of 86.5%–94.1%, with a PPV and NPV of 84.6%–90.9% and 78.6%–84.2%, respectively.

The PPV of this test in the real-world prospective cohorts is higher than other tests[31]; however, the NPV is relatively lower with a baseline disease prevalence of 50%–60%. This might be due to race differences. Compared with the Western practice, the Asian series exhibit a significantly higher ROM in most of the TBSRTC categories, whereas the resection rate was not statistically different reported by a meta-analysis,[32] indicating a higher ROM in surgically treated thyroid nodules in Asian series.[33] This is because diagnostic surgery is more frequently indicated for indeterminate nodules in Western thyroid nodule practice. Consequently, there is often a dilution of the ROM in surgically treated benign nodules reported in Western series.[33,34] Additionally, FNA is often indicated in Asian thyroid nodules with high TIRAD score nodules, which concentrate more malignant nodules in FNA specimens. Thus, there is a high ROM in all FNAs.[29] This results in a high baseline disease prevalence in the samples included in this study. Nevertheless, it is reassuring to note that 27 out of 28 false-negative cases identified in the study were confirmed as low-stage and low-risk cancers. Future research should include diverse populations to ensure the generalizability of findings, as single-race clinical studies may not fully represent the broader population.

Several molecular tests have been used for diagnosis of the benign and malignant disease of thyroid nodules. The most commonly studied gene panels include Afirma[5] and ThyroSeq,[19] which are based on DNA and RNA, as well as gene panels based on DNA methylation[35] and imprinted genes[23] that have been reported. Afirma achieved 100% sensitivity and 79.6% specificity, and ThyroSeq v.3 demonstrated 96.9% sensitivity and 84.8% specificity. These tests are more advanced than a simple and economic *BRAF* V600E test and offer benefits in diagnosing thyroid cancers without *BRAF* V600E mutation. Although commercially available panels such as Afirma and ThyroSeq have advanced the evaluation of thyroid nodules, they were developed and validated primarily in European and North American cohorts. Risk of malignancy,[33] mutational spectra,[28] and clinical management guidelines[7,30] for thyroid cancer differ between Western and Asian populations, limiting the direct transferability of these assays. To date, no molecular panel has been purpose-built and validated for Asian patients. ThyroProt fills this gap, offering a population-tailored solution that complements existing assays and, in the Asian clinical context, is indispensable for accurate risk stratification and informed decision-making. Rather than competing alternatives, these molecular diagnostic tools represent complementary approaches that can enhance thyroid nodule evaluation based on specific clinical needs and institutional capabilities, collectively advancing precision diagnosis in thyroid pathology.

Unlike existing molecular tests, this approach utilizes MS-based measurement of multiple proteins, introducing it to real-world clinical practice. This study introduces a protein test into the clinical arsenal, expanding the range of molecular tests used in thyroid nodules. This approach opens the possibility of developing a protein classifier, which could lead to even more accurate diagnosis of thyroid nodules in the future.

Compared to our previous study in which high-resolution mass spectrometers were used to discover novel protein classifiers,[26] this study adopts a relatively cost-effective, clinically accessible and practical approach, i.e., MRM-based targeted proteomics, to measure only the three selected proteins. In addition, we have synthesized stable isotope-labeled spike-in peptides as internal standards to achieve batch-independent absolute quantification, ensuring the best quality of quantification as a clinical test. We also have reduced the model panel from 19 proteins to 3 proteins and thereby decreased the LC gradient from 60 to 8 min, resulting in an almost 8-fold increase in throughput. There are two proteins that have been selected as model features in both this study and previous study, including fibronectin-1 (FN1) and heat shock protein beta-1 (HSPB1), which have been reported to be directly related to thyroid cancer.[36,37] The remaining protein also exhibits relevance to thyroid cancers. S100A6 has been reported to be significantly increased in PTC and independent of *BRAF* mutation.[38]

In this study, we have also included *BRAF* V600E, gender, and age as contributing features to enhance the model precision. In our prospective test cohorts, the prevalence of *BRAF* V600E mutations in malignant nodules was around 50%–80%, while in Bethesda III cytology it was around 20%–50% (Table 1). These prevalence rates are higher than the frequency observed in American cohorts[39,40] but consistent with Asian cohorts.[29,41]

The MS use in the present study is widely used in clinic for the measurement of small molecules, such as vitamins and drugs, but not yet widely applied for protein measurement in clinic

Table 3. Performance of the protein classifier (ThyroProt) on FNA samples of different Bethesda categories of thyroid nodule in the two independent prospective test sets

Variable	Independent test set 1						Independent test set 2	
	Bethesda II to VI nodules		Bethesda III to V nodules		Bethesda III & IV nodules		Bethesda II to VI nodules	
Protein classifier result	malignant	benign	malignant	benign	malignant	benign	malignant	benign
Malignant/positive, no.	120	12	50	5	7	5	11	2
Benign/negative, no.	21	77	11	52	2	48	6	32
AUC	0.91		0.89		0.93		0.87	
Accuracy, % (95% CI)	85.7 (85.5–85.8)		86.4 (86.2–86.6)		88.7 (88.4–89.0)		84.3 (83.8–84.8)	
Sensitivity, % (95% CI)	85.1 (79.2–91.0)		82.0 (72.3–91.6)		77.8 (50.6–100)		64.7 (42.0–87.4)	
Specificity, % (95% CI)	86.5 (79.4–93.6)		91.2 (83.9–98.6)		90.6 (82.7–98.4)		94.1 (86.2–100)	
PPV, % (95% CI)	90.9 (86.0–95.8)		90.9 (83.3–98.5)		58.3 (30.4–86.2)		84.6 (65.0–100)	
NPV, % (95% CI)	78.6 (70.4–86.7)		82.5 (73.2–91.9)		96.0 (90.6–100)		84.2 (72.6–95.8)	

although there is essentially no technical barrier.[42] This test can hardly be replaced by antibody-based test because the latter requires more sample amount and could not provide precise quantitative measurement for three proteins in a single test. In this prospective, noninterventional, multicenter study, we establish a protein classifier with a high sensitivity/NPV and high specificity/PPV for the diagnosis of thyroid nodules, including indeterminate thyroid nodules. This diagnostic approach can serve as both a rule-in and a rule-out test for thyroid malignancy in the clinical assessment of thyroid nodules. This study suggests feasibility and practicality of using targeted MS to detect multiple proteins for clinical diagnostics in real-world scenarios.

Limitations of the study

This study has several limitations. First, we substantially reduced the number of samples based on the original collection following strict inclusion criteria. This is a common practice of prospective studies. While ensuring diagnostic accuracy using the gold-standard approach, the reduced sample size may impact statistical power and limit immediate clinical applicability to all thyroid nodules. For model building and test, 393 benign samples were cytologically tested benign but lacked histopathological confirmation. But benign FNA diagnosis is generally highly accurate.[12,43] The diagnostic precision for separating Bethesda III and IV samples is lower than that for distinguishing Bethesda II and V and VI samples, probably due to the relatively lower number of samples in the III and IV groups. Future validation in larger cohort is required. The large number of participating medical centers was a strength of this multi-center study, but it could potentially be associated with data inhomogeneity. This was minimized by using the same criteria-based data collection protocol. Moreover, the tertiary medical centers participating in this study were equipped with highly skilled and modern medicine-driven physicians and pathologists, who played a crucial role in ensuring the reliability of the data. We included specimens from 17 medical centers in 11 cities, with the farthest two cities being 2,245 km apart. In China, there are significant differences in races and diets among different regions. Nevertheless, it would be necessary to perform future validations in more races, especially the Western populations considering the differences in population, malignancy rate, *BRAF* V600E mutation rate, and guidelines for diagnosis and management between Asia and the West. While MRM-based protein measurement may not yet match the convenience of PCR testing in current clinical settings, this practical limitation should not preclude its integration into future clinical applications. The exceptional value and reliability of MRM-based protein assays justify continued development. As these assays become more widely adopted, costs will decline and protocols will become increasingly streamlined, making routine clinical implementation increasingly feasible.

RESOURCE AVAILABILITY

Lead contact

Further information should be directed to and will be fulfilled by the lead contact, Tiannan Guo (guotiannan@westlake.edu.cn).

Materials availability

This study did not generate new unique reagents.

Data and code availability

- All the raw data have been deposited to the ProteomeXchange Consortium (http://proteomecentral.proteomexchange.org) via the PRIDE with the dataset identifier PXD046014.
- The code used in this study has been deposited at GitHub under https://github.com/guomics-lab/TPM.
- Any additional information required to reanalyze the data reported in this work paper is available from the lead contact upon request.

ACKNOWLEDGMENTS

Supported by the grants from the National Key R&D Program of China (no. 2022YFF0608403, 2021YFA1301600, and 2020YFE0202200), the National Natural Science Foundation of China (82072951 and 82122053), the Science and Technology Commission of Shanghai Municipality (22Y21900100 and 19DZ2251100), the Shanghai Anticancer Association (SACA-AX202213), the China Postdoctoral Science Foundation (2022M722841), Scientific Research and Development Fund of Zhongshan Hospital of Fudan University (2022ZSQD07), Shanghai Municipal Health Commission (SHSLCZDZK 03502), Applied Basic Research Program of Liaoning Province (2022020225-JH2/1013), CAMS Initiative for Innovative Medicine (2021-I2M-1–015), Key Area Research and Development Program of Guangdong Province (2021B0101420005), Shenzhen Science and Technology Program (ZDSYS20220606101604009), Shenzhen High-level Hospital Construction Fund, and Sanming Project of Medicine in Shenzhen (SZSM202211011). The funding sources had no role in the design and conduct of the study; collection, management, analysis of the data; preparation, review, or approval of the manuscript; and decision to submit the manuscript for publication.

AUTHOR CONTRIBUTIONS

T.G., Y.S., and X.C. conceived and designed the study. All authors were responsible for the acquisition, analysis, or interpretation and discussion of data. X.C., Y.S., Y. Zhu, and T.G. drafted the manuscript. All authors provided critical revision of the manuscript for important intellectual content. T.G., Y. Zhu, Y. Wang, H.X., H. Zhang, and Y.S. obtained funding. T.G. had full access to all of the data in the study and takes responsibility for the integrity of the data and the accuracy of the data analysis. We thank the patients and their families and caregivers for participating in the cohort; all the medical workers in the We-TEC Investigators for their support of this project; Drs. Jusheng Zheng and Oi Lian Kon for critical review of an earlier version of the manuscript; and Westlake University Supercomputer Center for assistance in data generation and storage.

DECLARATION OF INTERESTS

T.G. and Y. Zhu are shareholders of Westlake Omics Inc. W.G., L.T., L. Xu, Q.Z., and H. Si are employees of Westlake Omics Inc.

DECLARATION OF GENERATIVE AI AND AI-ASSISTED TECHNOLOGIES IN THE WRITING PROCESS

During the preparation of this work, the authors used ChatGPT in order to improve language and readability. After using this service, the authors reviewed and edited the content as needed and take full responsibility for the content of the publication.

STAR★METHODS

Detailed methods are provided in the online version of this paper and include the following:

- KEY RESOURCES TABLE
- EXPERIMENTAL MODEL AND STUDY PARTICIPANT DETAILS
  - Human samples
- METHOD DETAILS
  - Sample collection and storage
  - Ultrasound examination
  - Fine-needle aspiration
  - Cytopathology diagnoses
  - Histopathology
  - *BRAF* V600E mutation detection
  - Proteomics data acquisition
- QUANTIFICATION AND STATISTICAL ANALYSIS
  - Peptide quantification
  - Diagnostic model building
  - Feature selection
  - Statistical analysis

SUPPLEMENTAL INFORMATION

Supplemental information can be found online at https://doi.org/10.1016/j.xcrm.2026.102664.

Received: June 11, 2025
Revised: September 14, 2025
Accepted: February 11, 2026
Published: March 10, 2026

REFERENCES

1. Bray, F., Laversanne, M., Sung, H., Ferlay, J., Siegel, R.L., Soerjomataram, I., and Jemal, A. (2024). Global cancer statistics 2022: GLOBOCAN estimates of incidence and mortality worldwide for 36 cancers in 185 countries. CA Cancer J. Clin. *74*, 229–263. https://doi.org/10.3322/caac.21834.
2. Pizzato, M., Li, M., Vignat, J., Laversanne, M., Singh, D., La Vecchia, C., and Vaccarella, S. (2022). The epidemiological landscape of thyroid cancer worldwide: GLOBOCAN estimates for incidence and mortality rates in 2020. Lancet Diabetes Endocrinol. *10*, 264–272. https://doi.org/10.1016/S2213-8587(22)00035-3.
3. Chen, D.W., Lang, B.H.H., McLeod, D.S.A., Newbold, K., and Haymart, M.R. (2023). Thyroid cancer. Lancet *401*, 1531–1544. https://doi.org/10.1016/S0140-6736(23)00020-X.
4. Burman, K.D., and Wartofsky, L. (2015). CLINICAL PRACTICE. Thyroid Nodules. N. Engl. J. Med. *373*, 2347–2356. https://doi.org/10.1056/NEJMcp1415786.
5. Alexander, E.K., Kennedy, G.C., Baloch, Z.W., Cibas, E.S., Chudova, D., Diggans, J., Friedman, L., Kloos, R.T., LiVolsi, V.A., Mandel, S.J., et al. (2012). Preoperative diagnosis of benign thyroid nodules with indeterminate cytology. N. Engl. J. Med. *367*, 705–715. https://doi.org/10.1056/NEJMoa1203208.
6. Ali, S.Z., Baloch, Z.W., Cochand-Priollet, B., Schmitt, F.C., Vielh, P., and VanderLaan, P.A. (2023). The 2023 Bethesda System for Reporting Thyroid Cytopathology. Thyroid *33*, 1039–1044. https://doi.org/10.1089/thy.2023.0141.
7. Haugen, B.R., Alexander, E.K., Bible, K.C., Doherty, G.M., Mandel, S.J., Nikiforov, Y.E., Pacini, F., Randolph, G.W., Sawka, A.M., Schlumberger, M., et al. (2016). 2015 American Thyroid Association Management Guidelines for Adult Patients with Thyroid Nodules and Differentiated Thyroid Cancer: The American Thyroid Association Guidelines Task Force on Thyroid Nodules and Differentiated Thyroid Cancer. Thyroid *26*, 1–133. https://doi.org/10.1089/thy.2015.0020.
8. Medas, F., Dobrinja, C., Al-Suhaimi, E.A., Altmeier, J., Anajar, S., Arikan, A.E., Azaryan, I., Bains, L., Basili, G., Bolukbasi, H., et al. (2023). Effect of the COVID-19 pandemic on surgery for indeterminate thyroid nodules (THYCOVID): a retrospective, international, multicentre, cross-sectional study. Lancet Diabetes Endocrinol. *11*, 402–413. https://doi.org/10.1016/S2213-8587(23)00094-3.
9. Cibas, E.S., Baloch, Z.W., Fellegara, G., LiVolsi, V.A., Raab, S.S., Rosai, J., Diggans, J., Friedman, L., Kennedy, G.C., Kloos, R.T., et al. (2013). A prospective assessment defining the limitations of thyroid nodule pathologic evaluation. Ann. Intern. Med. *159*, 325–332. https://doi.org/10.7326/0003-4819-159-5-201309030-00006.
10. Vaccarella, S., Franceschi, S., Bray, F., Wild, C.P., Plummer, M., and Dal Maso, L. (2016). Worldwide Thyroid-Cancer Epidemic? The Increasing Impact of Overdiagnosis. N. Engl. J. Med. *375*, 614–617. https://doi.org/10.1056/NEJMp1604412.
11. Eszlinger, M., Lau, L., Ghaznavi, S., Symonds, C., Chandarana, S.P., Khalil, M., and Paschke, R. (2017). Molecular profiling of thyroid nodule fine-needle aspiration cytology. Nat. Rev. Endocrinol. *13*, 415–424. https://doi.org/10.1038/nrendo.2017.24.
12. Alexander, E.K., and Cibas, E.S. (2022). Diagnosis of thyroid nodules. Lancet Diabetes Endocrinol. *10*, 533–539. https://doi.org/10.1016/S2213-8587(22)00101-2.
13. Xing, M., Alzahrani, A.S., Carson, K.A., Viola, D., Elisei, R., Bendlova, B., Yip, L., Mian, C., Vianello, F., Tuttle, R.M., et al. (2013). Association between BRAF V600E mutation and mortality in patients with papillary thyroid cancer. JAMA *309*, 1493–1501. https://doi.org/10.1001/jama.2013.3190.
14. Xing, M. (2013). Molecular pathogenesis and mechanisms of thyroid cancer. Nat. Rev. Cancer *13*, 184–199. https://doi.org/10.1038/nrc3431.
15. Jinih, M., Foley, N., Osho, O., Houlihan, L., Toor, A.A., Khan, J.Z., Achakzai, A.A., and Redmond, H.P. (2017). BRAFV600E mutation as a predictor of thyroid malignancy in indeterminate nodules: A systematic review and meta-analysis. Eur. J. Surg. Oncol. *43*, 1219–1227. https://doi.org/10.1016/j.ejso.2016.11.003.
16. Fu, G., Chazen, R.S., Monteiro, E., Vescan, A., Freeman, J.L., Witterick, I.J., and MacMillan, C. (2023). Facilitation of Definitive Cancer Diagnosis With Quantitative Molecular Assays of BRAF V600E and TERT Promoter

Variants in Patients With Thyroid Nodules. JAMA Netw. Open *6*, e2323500. https://doi.org/10.1001/jamanetworkopen.2023.23500.

17. Chudova, D., Wilde, J.I., Wang, E.T., Wang, H., Rabbee, N., Egidio, C.M., Reynolds, J., Tom, E., Pagan, M., Rigl, C.T., et al. (2010). Molecular classification of thyroid nodules using high-dimensionality genomic data. J. Clin. Endocrinol. Metab. *95*, 5296–5304. https://doi.org/10.1210/jc.2010-1087.
18. Patel, K.N., Angell, T.E., Babiarz, J., Barth, N.M., Blevins, T., Duh, Q.Y., Ghossein, R.A., Harrell, R.M., Huang, J., Kennedy, G.C., et al. (2018). Performance of a Genomic Sequencing Classifier for the Preoperative Diagnosis of Cytologically Indeterminate Thyroid Nodules. JAMA Surg. *153*, 817–824. https://doi.org/10.1001/jamasurg.2018.1153.
19. Nikiforova, M.N., Wald, A.I., Roy, S., Durso, M.B., and Nikiforov, Y.E. (2013). Targeted next-generation sequencing panel (ThyroSeq) for detection of mutations in thyroid cancer. J. Clin. Endocrinol. Metab. *98*, E1852–E1860. https://doi.org/10.1210/jc.2013-2292.
20. Nikiforov, Y.E., Carty, S.E., Chiosea, S.I., Coyne, C., Duvvuri, U., Ferris, R.L., Gooding, W.E., LeBeau, S.O., Ohori, N.P., Seethala, R.R., et al. (2015). Impact of the Multi-Gene ThyroSeq Next-Generation Sequencing Assay on Cancer Diagnosis in Thyroid Nodules with Atypia of Undetermined Significance/Follicular Lesion of Undetermined Significance Cytology. Thyroid *25*, 1217–1223. https://doi.org/10.1089/thy.2015.0305.
21. Valderrabano, P., Khazai, L., Leon, M.E., Thompson, Z.J., Ma, Z., Chung, C.H., Hallanger-Johnson, J.E., Otto, K.J., Rogers, K.D., Centeno, B.A., and McIver, B. (2017). Evaluation of ThyroSeq v2 performance in thyroid nodules with indeterminate cytology. Endocr. Relat. Cancer *24*, 127–136. https://doi.org/10.1530/ERC-16-0512.
22. Steward, D.L., Carty, S.E., Sippel, R.S., Yang, S.P., Sosa, J.A., Sipos, J.A., Figge, J.J., Mandel, S., Haugen, B.R., Burman, K.D., et al. (2019). Performance of a Multigene Genomic Classifier in Thyroid Nodules With Indeterminate Cytology: A Prospective Blinded Multicenter Study. JAMA Oncol. *5*, 204–212. https://doi.org/10.1001/jamaoncol.2018.4616.
23. Xu, H., Zhang, Y., Wu, H., Zhou, N., Li, X., Pineda, J.P., Zhu, Y., Fu, H., Ying, M., Yang, S., et al. (2023). High Diagnostic Accuracy of Epigenetic Imprinting Biomarkers in Thyroid Nodules. J. Clin. Oncol. *41*, 1296–1306. https://doi.org/10.1200/JCO.22.00232.
24. Guo, T., Kouvonen, P., Koh, C.C., Gillet, L.C., Wolski, W.E., Röst, H.L., Rosenberger, G., Collins, B.C., Blum, L.C., Gillessen, S., et al. (2015). Rapid mass spectrometric conversion of tissue biopsy samples into permanent quantitative digital proteome maps. Nat. Med. *21*, 407–413. https://doi.org/10.1038/nm.3807.
25. Cai, X., Xue, Z., Wu, C., Sun, R., Qian, L., Yue, L., Ge, W., Yi, X., Liu, W., Chen, C., et al. (2022). High-throughput proteomic sample preparation using pressure cycling technology. Nat. Protoc. *17*, 2307–2325. https://doi.org/10.1038/s41596-022-00727-1.
26. Sun, Y., Selvarajan, S., Zang, Z., Liu, W., Zhu, Y., Zhang, H., Chen, W., Chen, H., Li, L., Cai, X., et al. (2022). Artificial intelligence defines protein-based classification of thyroid nodules. Cell Discov. *8*, 85. https://doi.org/10.1038/s41421-022-00442-x.
27. Kettenbach, A.N., Rush, J., and Gerber, S.A. (2011). Absolute quantification of protein and post-translational modification abundance with stable isotope–labeled synthetic peptides. Nat. Protoc. *6*, 175–186. https://doi.org/10.1038/nprot.2010.196.
28. Kakudo, K. (2022). Different Threshold of Malignancy for RAS-like Thyroid Tumors Causes Significant Differences in Thyroid Nodule Practice. Cancers (Basel) *14*, 812. https://doi.org/10.3390/cancers14030812.
29. Zhu, Y., Wu, H., Huang, B., Shen, X., Cai, G., and Gu, X. (2020). BRAF(V600E) mutation combined with American College of Radiology thyroid imaging report and data system significantly changes surgical resection rate and risk of malignancy in thyroid cytopathology practice. Gland Surg. *9*, 1674–1684. https://doi.org/10.21037/gs-20-535.
30. Chinese Society of Endocrinology; Thyroid and Metabolism Surgery Group of the Chinese Society of Surgery; China Anti-Cancer Association, Chinese Association of Head and Neck Oncology; Chinese Society of Nuclear Medicine; China Anti-Cancer Association, Chinese Association of Thyroid Oncology; Chinese Thyroid Association, Chinese Collage of Surgeons, Chinese Medical Doctor Association; Chinese Medical Doctor Association; Chinese Society of Ultrasound in Medicine (2023). Guidelines for the diagnosis and management of thyroid nodules and differentiated thyroid cancer (Second edition). Chinese Journal of Endocrinology and Metabolism *39*, 3.
31. Livhits, M.J., Zhu, C.Y., Kuo, E.J., Nguyen, D.T., Kim, J., Tseng, C.H., Leung, A.M., Rao, J., Levin, M., Douek, M.L., et al. (2021). Effectiveness of Molecular Testing Techniques for Diagnosis of Indeterminate Thyroid Nodules: A Randomized Clinical Trial. JAMA Oncol. *7*, 70–77. https://doi.org/10.1001/jamaoncol.2020.5935.
32. Ooi, L.Y., and Nga, M.E. (2020). Atypia of undetermined significance/follicular lesion of undetermined significance: Asian vs. non-Asian practice, and the Singapore experience. Gland Surg. *9*, 1764–1787. https://doi.org/10.21037/gs-20-555.
33. Vuong, H.G., Ngo, H.T.T., Bychkov, A., Jung, C.K., Vu, T.H., Lu, K.B., Kakudo, K., and Kondo, T. (2020). Differences in surgical resection rate and risk of malignancy in thyroid cytopathology practice between Western and Asian countries: A systematic review and meta-analysis. Cancer Cytopathol. *128*, 238–249. https://doi.org/10.1002/cncy.22228.
34. Kakudo, K., Higuchi, M., Hirokawa, M., Satoh, S., Jung, C.K., and Bychkov, A. (2017). Thyroid FNA cytology in Asian practice-Active surveillance for indeterminate thyroid nodules reduces overtreatment of thyroid carcinomas. Cytopathology *28*, 455–466. https://doi.org/10.1111/cyt.12491.
35. Park, J.L., Jeon, S., Seo, E.H., Bae, D.H., Jeong, Y.M., Kim, Y., Bae, J.S., Kim, S.K., Jung, C.K., and Kim, Y.S. (2020). Comprehensive DNA Methylation Profiling Identifies Novel Diagnostic Biomarkers for Thyroid Cancer. Thyroid *30*, 192–203. https://doi.org/10.1089/thy.2019.0011.
36. Sponziello, M., Rosignolo, F., Celano, M., Maggisano, V., Pecce, V., De Rose, R.F., Lombardo, G.E., Durante, C., Filetti, S., Damante, G., et al. (2016). Fibronectin-1 expression is increased in aggressive thyroid cancer and favors the migration and invasion of cancer cells. Mol. Cell. Endocrinol. *431*, 123–132. https://doi.org/10.1016/j.mce.2016.05.007.
37. Li, Y., Yang, Q., Guan, H., Shi, B., Ji, M., and Hou, P. (2018). ZNF677 Suppresses Akt Phosphorylation and Tumorigenesis in Thyroid Cancer. Cancer Res. *78*, 5216–5228. https://doi.org/10.1158/0008-5472.CAN-18-0003.
38. Sofiadis, A., Dinets, A., Orre, L.M., Branca, R.M., Juhlin, C.C., Foukakis, T., Wallin, G., Höög, A., Hulchiy, M., Zedenius, J., et al. (2010). Proteomic Study of Thyroid Tumors Reveals Frequent Up-Regulation of the Ca2+-Binding Protein S100A6 in Papillary Thyroid Carcinoma. Thyroid *20*, 1067–1076. https://doi.org/10.1089/thy.2009.0400.
39. Cancer Genome Atlas Research Network (2014). Integrated genomic characterization of papillary thyroid carcinoma. Cell *159*, 676–690. https://doi.org/10.1016/j.cell.2014.09.050.
40. Chiosea, S., Hodak, S.P., Yip, L., Abraham, D., Baldwin, C., Baloch, Z., Gulec, S.A., Hannoush, Z.C., Haugen, B.R., Joseph, L., et al. (2023). Molecular Profiling of 50 734 Bethesda III-VI Thyroid Nodules by ThyroSeq v3: Implications for Personalized Management. J. Clin. Endocrinol. Metab. *108*, 2999–3008. https://doi.org/10.1210/clinem/dgad220.
41. Chen, H., Song, A., Wang, Y., He, Y., Tong, J., Di, J., Li, C., Zhou, Z., Cai, X., Zhong, D., and Da, J. (2022). BRAF(V600E) mutation test on fine-needle aspiration specimens of thyroid nodules: Clinical correlations for 4600 patients. Cancer Med. *11*, 40–49. https://doi.org/10.1002/cam4.4419.
42. Schiess, R., Wollscheid, B., and Aebersold, R. (2009). Targeted proteomic strategy for clinical biomarker discovery. Mol. Oncol. *3*, 33–44. https://doi.org/10.1016/j.molonc.2008.12.001.

43. Cibas, E.S., and Ali, S.Z. (2017). The 2017 Bethesda System for Reporting Thyroid Cytopathology. Thyroid *27*, 1341–1346. https://doi.org/10.1089/thy.2017.0500.

44. Rost, H.L., Sachsenberg, T., Aiche, S., Bielow, C., Weisser, H., Aicheler, F., Andreotti, S., Ehrlich, H.C., Gutenbrunner, P., Kenar, E., et al. (2017). OpenMS: a flexible open-source software platform for mass spectrometry data analysis. Nat. Methods *13*, 741–748. https://doi.org/10.1038/nmeth.3959.

45. Sun, Y., Li, L., Zhou, Y., Ge, W., Wang, H., Wu, R., Liu, W., Chen, H., Xiao, Q., Cai, X., et al. (2022). Stratification of follicular thyroid tumours using data-independent acquisition proteomics and a comprehensive thyroid tissue spectral library. Mol. Oncol. *16*, 1611–1624. https://doi.org/10.1002/1878-0261.13198.

STAR★METHODS

KEY RESOURCES TABLE

REAGENT or RESOURCE	SOURCE	IDENTIFIER
Biological samples		
FNA samples	14 clinical centers	This paper (Table S1)
Chemicals, peptides, and recombinant proteins		
Ammonium bicarbonate buffer (ABB)	General-Reagent	Cat #G12990A
Heptane	Sigma-Aldrich	Cat # 246654-2L
Hydroxylamine	Thermo Scientific	Cat # 90115
Tris Base	Promega	Cat #H5133
Urea	Sigma-Aldrich	Cat #U1250
Thiourea	Sigma-Aldrich	Cat #T8656-500G
Tris (2-carboxyethyl) phosphine (TCEP)	Adamas-beta	Cat # 61820E
Iodoacetamide (IAA)	Sigma-Aldrich	Cat #I6125
Trypsin	Hualishi Tech	Cat # HLS TRY001C
Lys-C	Hualishi Tech	Cat # HLS LYS001C
Trifluoroacetic acid (TFA)	Thermo Fisher Scientific	Cat # 85183
Water	Thermo Fisher Scientific	Cat #W6-4
Acetonitrile	Thermo Fisher Scientific	Cat # A955-4
Formic acid (FA)	Thermo Fisher Scientific	Cat # A117-50
Ammonium hydroxide solution	Sigma-Aldrich	Cat # 221228
Methanol	Sigma-Aldrich	Cat # 34860
Critical commercial assays		
QIAamp DNA Micro Kit	QIAGEN	Cat # 56304
BRAF V600E ARMS-PCR Kit	AmoyDx	Cat # 20143401824
Deposited data		
Mass spectrometry data	This paper	ProteomeXchange Consortium: PXD046014
Software and algorithms		
Analyst MD 1.6.3	AB SCIEX	https://sciex.com/products/in-vitro-diagnostics/enhancements-and-options/analyst-md-software
R version 4.2.1	R Project	https://www.r-project.org
OpenMS 2.4.0	Röst et al.[44]	https://openms.de/
Other		
SOLAμ	Thermo Fisher Scientific	Cat # 62209-001
Hypersil GOLD column,100*2.1 mm, 1.9 μm	Thermo Fisher Scientific	Cat # 25002-102130

EXPERIMENTAL MODEL AND STUDY PARTICIPANT DETAILS

Human samples

This study was approved by the ethics committees of Fudan University Shanghai Cancer Center (2207257-15), Shanghai Tenth People's Hospital (SHYS-IEC-5.0/22K210/P01), Affiliated Hangzhou First People's Hospital (2019-040-01), the First Hospital of China Medical University (2019-280-2), Zhongshan Hospital of Fudan (B2022-370(2)), Beijing Aerospace General Hospital (2022-118), Wuhan University Renmin Hospital (2019K-K103(J01)), Zhejiang Cancer Hospital (IRB-2023-842), Sir Run Run Show Hospital (LXSHYJ-20221122-01) and Westlake University (20231106GTN001). All patients involved in the study provided informed consent to participate. Cytologists/pathologists were unaware of the molecular analysis results, and the molecular analyses were independent of the cytology and histopathology results. All authors contributed to data interpretation and manuscript preparation and vouch for the completeness and accuracy of the data and for the fidelity of the study protocol.

This was a prospective, noninterventional, multicenter study involving patients who had ultrasonographically confirmed thyroid nodules. Both patients and physicians were blinded to the results of the classifier. FNA samples were collected from patients at 17 tertiary medical centers in China (Table S1). Each sample represented a single FNA needle pass per nodule. FNA needle specifications are provided in the method details. The inclusion criteria include: 1) Untreated patients with initial thyroid nodules, 2) Undergoing thyroid nodules fine needle aspiration, 3) Bethesda assessment information, 4) Patients voluntarily participating in the study after informed consent. The exclusion criteria include: 1) without thyroid nodules fine needle aspiration, 2) Insufficient number of cells in the fine needle aspiration sample of the thyroid. Gender was incorporated as one of the features in our predictive model. Therefore, gender does not confound the study results, as its influence has been accounted for in the classifier.

METHOD DETAILS

Sample collection and storage

Prospective fine needle aspiration (FNA) samples for molecular analysis were obtained *in vivo* during outpatient clinical visits. The FNA procedure involved one or two passes, and the samples were immediately transferred into FNAprotect preservative solution. After collection, the samples were shipped frozen in dry ice to Westlake University. The molecular testing on FNA samples was conducted in a blinded manner, without knowledge of the clinical, cytologic, and histopathologic diagnoses.

Ultrasound examination

All ultrasound examinations were performed using a linear-array probe (Logiq E9, GE Healthcare, Wauwatosa, WI, USA) by experienced radiologists in thyroid imaging. Observe the thyroid nodules from multiple perspectives, such as transverse and longitudinal sections. Observational indicators include: age, longitudinal-to-transverse ratio, echogenicity, calcification, margin, composition, relationship with the capsule, size, location, and number of lesions. Calcification can be classified as: no calcification, microcalcifications (long diameter < 2mm), coarse calcifications (long diameter > 2mm), and peripheral rim calcifications. Record using the ACR TI-RADS system.

Fine-needle aspiration

FNA was usually performed to nodules with relatively high-grade ACR TI-RADS categories and other clinical risk indications. All FNAs were conducted by experienced radiologists under ultrasound guidance. For each thyroid nodule, FNA was performed at the skin superficial under ultrasound guidance using a 5-mL plastic disposable syringe with a 22-gauge needle. A portion of the FNA specimen was smeared onto glass slides and fixed with 95% alcohol for cytopathology analysis; Partially was expelled into the cell preservation solution and refrigerate or freeze for related *BRAF* V600E mutation detection and proteomic analysis.

Cytopathology diagnoses

Following FNA, local cytology reports were collected for all subjects. The interpretation process was jointly carried out by two experienced pathologists. According to the Bethesda reporting system,[43] thyroid nodules are classified into six diagnostic categories: (I) nondiagnostic or unsatisfactory, Specimens contain <6 follicular cell clusters, and each cluster contains <10 cells.; (II) benign; (III) atypia of undetermined significance or follicular lesion of undetermined significance; (IV) follicular neoplasm or suspicious for a follicular neoplasm; (v) suspicious for malignancy; and (V) malignant. Among them, Samples classified as Bethesda III to V are indeterminate thyroid nodules that are difficult to diagnose.

Histopathology

Following surgery, local histopathology reports and slides were collected and biopsied nodules were matched to resected nodules by size and location. All slides were independently evaluated by two experienced specialist pathologists. More pathologists were involved until a consensus was reached in cases of discrepant pathological diagnoses. Throughout the study, all pathologists were unaware of local histopathology diagnosis and molecular test results.

BRAF V600E mutation detection

DNA was extracted from FNA specimens using the QIAamp DNA Micro Kit from Qiagen, Germany. *BRAF* V600E mutation status was determined using the Human *BRAF* V600E ARMS-PCR Kit from Xiamen Aide Pharmaceutical Technology Co., Ltd.

Proteomics data acquisition

Peptides were extracted from the FNA samples as previously described.[25,26] Briefly, the FNA sample was collected in red blood cell lysis buffer followed by centrifugation to remove red blood cells. Proteins then were extracted using a lysis buffer containing 6 M urea and 2 M thiourea in 100 mM ammonium bicarbonate buffer (ABB) with assistance from pressure cycling technology (PCT). Following extraction, the proteins were subjected to reduction and alkylation using 20 mM Tris (2-carboxyethyl) phosphine (TCEP) and 40 mM iodoacetamide (IAA). Subsequently, PCT-assisted enzymatic digestion was carried out by adding Lys-C (enzyme-to-substrate ratio, 1:80) and trypsin (enzyme-to-substrate ratio, 1:20) to the foregoing mixture. Finally, peptides were cleaned using C18 solid phase extraction (SPE) columns before mass spectrometry (MS) analysis. Peptide samples for first feature selection were analyzed by multiple reaction monitoring (MRM) mass spectrometry in TRIPLE QUADTM 4500MD (SCIEX, CA, USA) coupled with Jasper^{TM} high

performance liquid chromatography (HPLC) system (SCIEX, CA, USA). A total of 179 peptides from 122 proteins were acquired by 20-min liquid chromatography with tandem mass spectrometry (LC-MS/MS) methods at a flow rate of 0.2 mL/min. Peptide samples mixed with synthesized stable isotope labeled peptides (called AQUA peptides)[27] for second feature selection, model training and validation were analyzed over an 20-min and 8-min LC gradient. In the case of the independent test set, three peptides coupled with AQUA peptides were analyzed using an 8-minute LC gradient. The MS data were analyzed using OpenMS (version 2.6.0).[44] All the training set, validation set and test set samples in this study were collected for protein data based on MS.

QUANTIFICATION AND STATISTICAL ANALYSIS

Peptide quantification

The OpenSwathAssayGenerator module was employed for library file filtering and optimization. Initially, all transitions were annotated based on predefined standards. Subsequently, transitions were filtered using a minimum quantity threshold of 0.1 to enhance peptide detection sensitivity. This process generated a TraML format file for standardized exchange and transfer of transition list data. The MRMMapper module was employed to match mzML format MRM data against a TraML library file containing Decoys. A precursor ion tolerance of 1 was set, and a multi-mapping algorithm was used to match one or more mapping targets for the chromatograms in the mzML format, resulting in an annotated.mzML file. The OpenSwathAnalyzer module was utilized to perform peak picking on the mzML file containing mapping metadata based on a TraML library file containing Decoys, using a non-strict mode. Scoring was conducted to obtain proteomics data, resulting in a featureXML format file. The OpenSwathFeatureXMLToTSV module was used to generate readable tsv files based on featureXML and the TraML library file containing Decoys. The maximum peak area for each peptide segment corresponds to the peptide information. For labeled peptide determination, doubly labeled peptides were prioritized when multiple labeled peptides were present. Among remaining candidates, peptides with the highest intensity were selected. For light-labeled (unlabeled) peptide determination, the precursor ion with retention time closest to the corresponding heavy label was selected. If the retention time difference exceeded a predefined threshold (x), the light label intensity was assigned as zero. The threshold x was determined by calculating the retention time deviation between heavy and light labels across all pool samples, using three times the interquartile range (IQR), which yielded x = 1.59 seconds.

Diagnostic model building

To optimize the model's performance under the new logistic regression framework, a series of critical parameter adjustments were undertaken. A concise summary of these modifications includes: Cross-Validation Strategy, Regularization Strength (C), Penalty Type, Solver, Maximum Iterations.

The hyperparameters for the logistic regression model were optimized using grid search. The regularization parameter (C) was tested across a range from 0.001 to 10.0, including values of 0.001, 0.01, 0.05, 0.1, 0.2, 0.3, and incrementally up to 10.0. Both L1 and L2 penalty terms were evaluated. The liblinear solver was employed for optimization. The maximum number of iterations was tested at 100, 1000, 5000, and 10,000 to ensure model convergence. A transition to logistic regression entailed a reevaluation of the modeling approach. Employing five-fold cross-validation on the training dataset, the focus shifted to identifying the most effective parameter configuration based on maximized predictive accuracy. The optimal setting identified was characterized by a regularization strength (C) of 0.05, an L2 penalty for regularization, the 'liblinear' solver for optimization, and a maximum of 100 iterations for convergence. Leveraging this optimal parameter combination, the model was reconstructed utilizing the entirety of the training dataset, ensuring a robust and accurate predictive framework. The well-established model was employed to make predictions in several test sets.

Feature selection

Based on previous studie[26,45] and the clinically available immunohistochemistry (IHC)-detected proteins, 211 proteins were selected as candidate diagnostic biomarkers. After optimization, a total of 121 proteins could be successfully validated using MRM-MS. 820 MRM-MS data for 620 samples were used for the first round of machine learning-based feature selection (Table S2A). 1312 MRM-MS data for 1312 samples mixed AQUA peptides were used for the second round of machine learning-based feature selection (Tables S2B and S2C). After multiple rounds of protein biomarker screening, including MRM optimization, machine learning model screening, evaluation of AQUA peptides stability and linearity, and MS signal screening, three proteins were ultimately selected as the final features of the classifier model (ThyroProt).

Statistical analysis

To augment the predictive capability of the analysis, logistic regression, implemented via the scikit-learn library (version 1.0.2), was employed with a focus on optimizing pivotal parameters through a five-fold cross-validation strategy. Specifically, the regularization strength (C) was calibrated to 0.05, favoring models with more restrained coefficients to guard against overfitting. An L2 penalty was selected to penalize the squared magnitude of the coefficients, thereby enhancing model stability. The 'liblinear' solver was adopted for its demonstrated efficacy in handling datasets of smaller dimensions alongside L2 penalties. Lastly, a maximum of 100 iterations (max_iter) was established, ensuring the solver was provided ample opportunity to converge toward an optimal solution. The receiver operating characteristic curve (ROC) analysis, accuracy, sensitivity, specificity, positive predictive value (PPV), and negative predictive value (NPV) were used to determine the diagnostic utility of the classifier model.